FEM ANALYSIS OF STRESS AND STRAIN STATE OF A WORM FACE-GEAR WITH REVERSE TAPERED PINION

Ligia Cristina Brezeanu, Bogdan Bucur
Petru Maior University, Tg. Mures, Romania
brezeanu@upm.ro, bbogdan@upm.ro

ABSTRACT

In this paper an analysis of stresses and strains of the condition of a worm face-gear with reverse tapered pinion. The study is performed by FEM analysis.

Keywords: Worm-Face Gear, Reverse tapered, FEM analysis, Finite Element, Stresses, Displacements

1. Theoretical aspects

The worm face-gear (Fig.1.) belonging to the group of gear with cross axis is defined as a worm face-gear with reverse taper pinion.

Compared to the other gears these face-gear presented many constructive and functional advantages: increased bearing force to general-purpose worm gear which makes them to be sensitive overall dimensions smaller, contact line incomparably high coverage, good lubrication conditions, higher ratios, increased accuracy and quiet operation.

Due to the particular geometry of worm face-gear with reverse taper pinion - the flanks of worm being strongly asymmetric approach, allows the absolute control of the backlash, the axial displacement of a worm or screw worm-wheel.

The characteristic geometry elements of a worm face-gear with reverse tapered are presented in Fig 2.

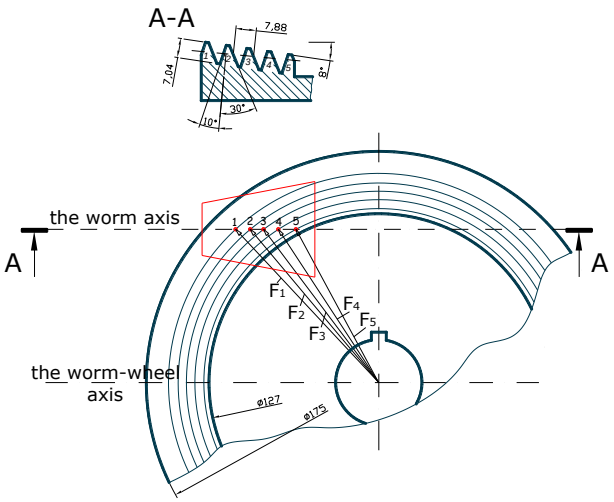

Fig. 2. The constructive geometry of worm face-gear. The contact position of worm-wheel in operation

Fig. 1. The worm face-gear with reverse tapered pinion

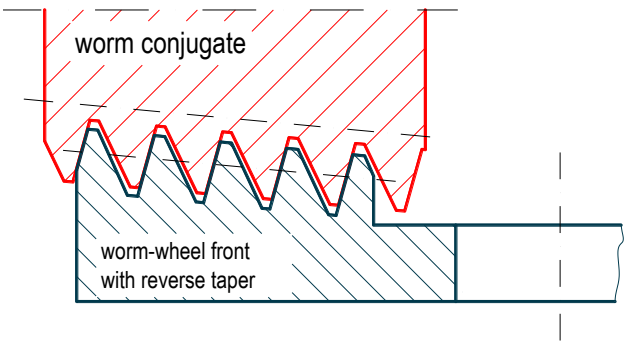

Fig.3. Section through the worm worm-wheel; the bearing flank 10^0

.

2. Modeling and meshing

Having analyzed the studied structure, it was found that a correct interpretation of the phenomenon of contact between worm-worm wheels can be seen in axial section plan between the two elements of face-gear (Fig. 2).

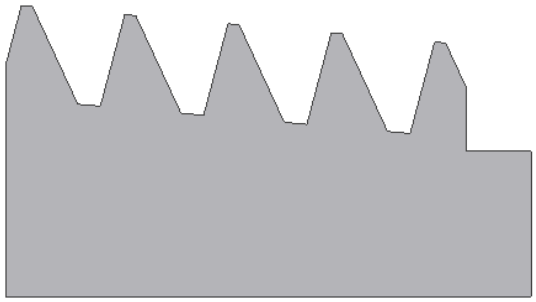

Fig. 4. Modeling – Inventor 10

Geometric data corresponding section of the plan was made in program design modeling Inventor.10 (Fig. 4) and then made the transfer to ALGOR V16 Fempro analysis program (Fig.5).

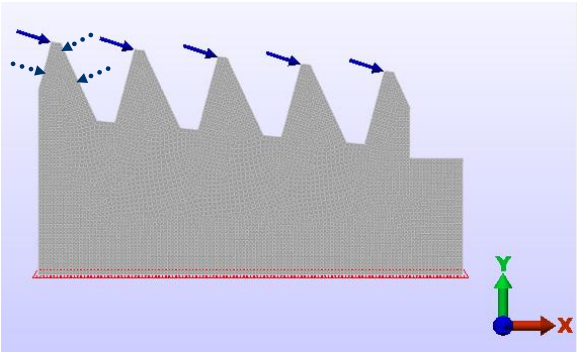

Fig.5. Meshing – Loads - Constraints

Finite elements used are type 2D - two-dimensional quadrilateral and triangular After meshing result:

a. Number of nodes : 12,989
b. Number E.F.- type 2D: 13,042

Nodal boundary conditions are fixed in the nodes of the worm-wheel.

The features elastic material of wheel which is by: ERTACETAL C, the elastic characteristics: E = 3600 N/mm^2, μ = 0.4 [7].

The loading flank's was done by calculating the forces corresponding to the 5 points of contact between teeth of worm-wheel in contact with the conjugated surface of the worm (Fig.3).

The torque transmitted of the worm-wheel M_t was calculating with relationship:

$$M_t = 9{,}55.10^6 \frac{P}{n} \; [N.mm] \qquad (1)$$

Which:

- P - power [kW];
- n - speed [r.p.m];

On the other hand the torque transmitted M_t is:

$$M_t = F.\frac{d}{2} \qquad (2)$$

Which:

- F - force in contact point of worm-worm-wheel [N];
- d - diameter of contact point corresponding for each tooth of the worm wheel;

$$\Rightarrow \quad F = \frac{2}{d}.9{,}55.10^6 \frac{P}{n} \; [N] \qquad (3)$$

Considered the following corresponding to experimental values:

P = 1,5 kW and n = 1500 rpm input speed, gear ratio i =1:47, axial distance A = 58mm, module m_a = 2,5mm, bearing flank angle α_1=10°, support flank angle α_2=30°, Archimedes worm type reverse tapered, δ_1=5°, reverse tapered worm-wheel drive δ_2=8°.

Thus, corresponding the diameter of contact points of five teeth of worm-wheel results:

1 - d_1 = 158,35 mm $\Rightarrow$ F_1 = 120,62 N
2 - d_2 = 151,06 mm $\Rightarrow$ F_2 = 126,44 N
3 - d_3 = 144,84 mm $\Rightarrow$ F_3 = 131,87 N
4 - d_4 = 138,46 mm $\Rightarrow$ F_4 = 137,95 N
5 - d_5 = 131,70 mm $\Rightarrow$ F_5 = 145,03 N

Constructive and functional reasons, the tooth five is considered a hard drive smaller force than that calculated, namely: F_5 = 130,5 N.

3. Results

The results are considered to be significant for the interpretation and relevance given the phenomenon studied, are the values:

- Stress by Von Mises equivalent theory $\sigma_{ech;}$
- Minimal by main stress σ_2 (with compression effect);
- Resultant structure shift. Displacement.

They studied four cases of loading:

Case I - load bearing flank to 10^0:
a) Entry into gear
b) Loading in operating
Case II - load bearing flank to 30^0:
a) Entry into gear
b) Loading in operating

On the simulations performed were obtained the following results:

Case I - load bearing flank to 10^0:

a) Entry into gear

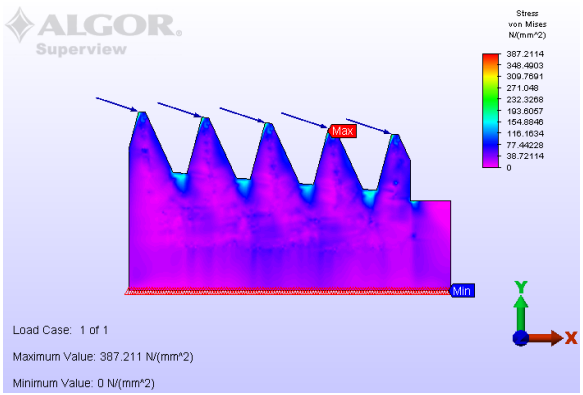

Fig. 6. Equivalent Von Mises stress distribution

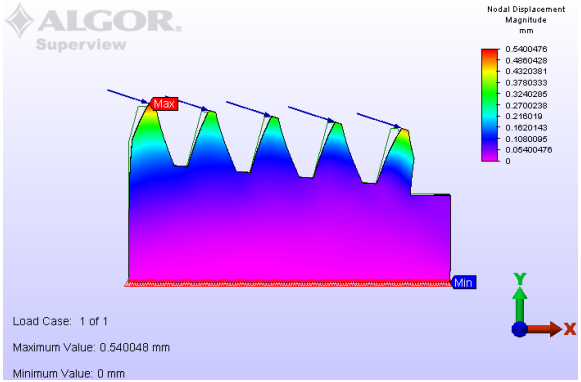

Fig. 9. Displacement distribution – areas of equal displacement. Deformed position of the structure

b) Loading in operating

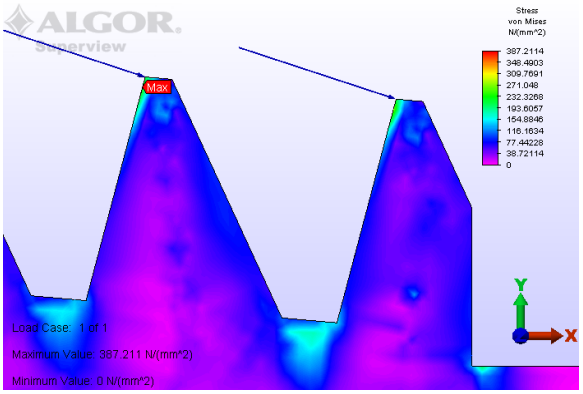

Fig. 7. Detail – Equivalent Von Mises stress distribution in area with high application

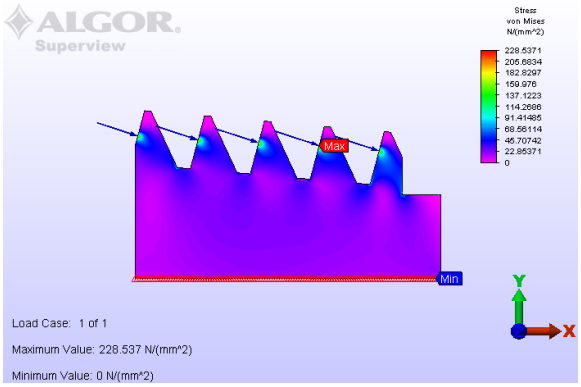

Fig. 10. Equivalent Von Mises stress distribution

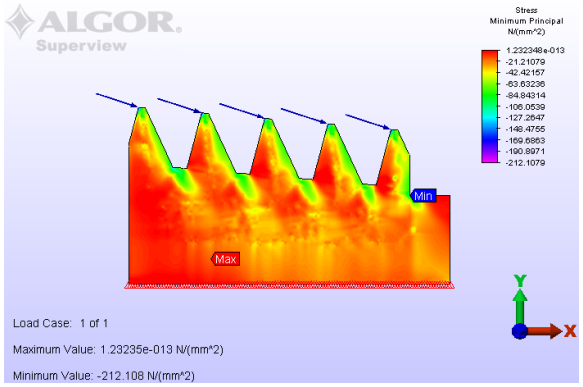

Fig. 8. Minimum principal stress distribution (compressive stress distribution)

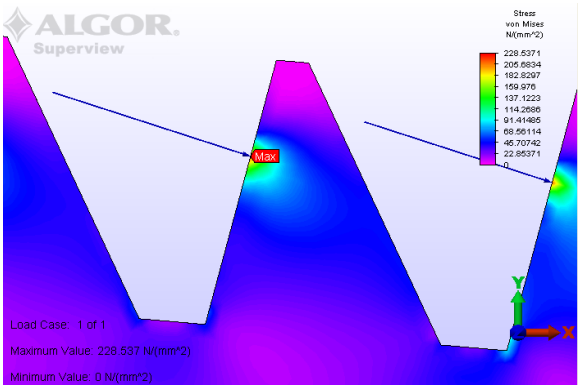

Fig. 11. Detail – Equivalent Von Mises stress distribution in area with high application

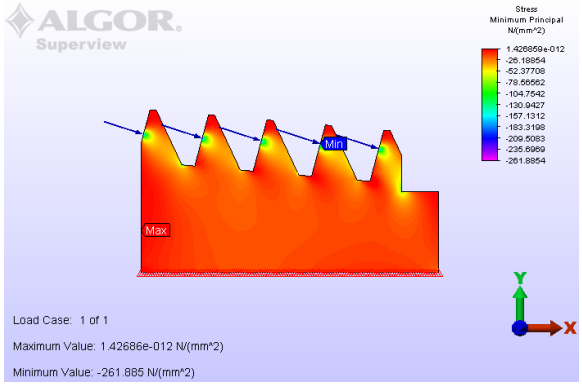

Fig. 12. Minimum principal stress distribution (compressive stress distribution)

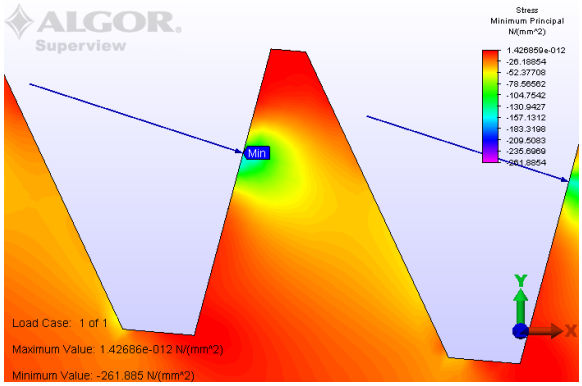

Fig. 13. Detail – Minimum principal stress distribution in area with high application

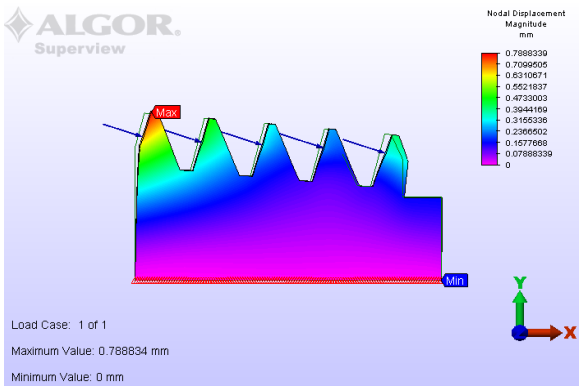

Fig. 14. Displacement distribution – areas of equal displacement. Deformed position of the structure

Case II - load bearing flank to 30^0:

a) Entry into gear

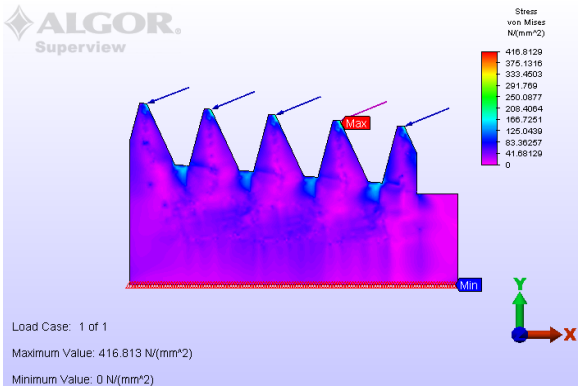

Fig. 15. Equivalent Von Mises stress distribution

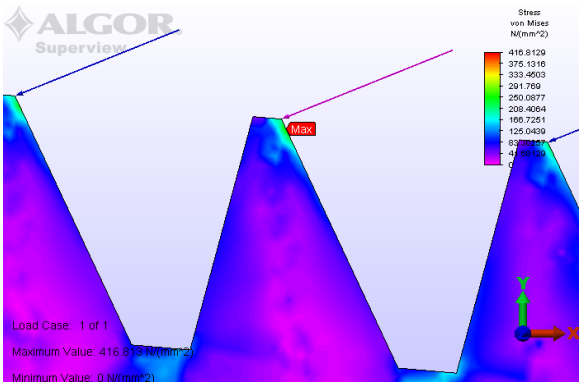

Fig. 16. Detail – Equivalent Von Mises stress distribution in area with high application

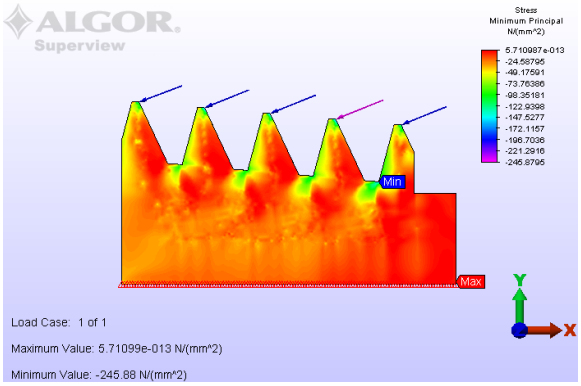

Fig. 17. Minimum principal stress distribution (compressive stress distribution)

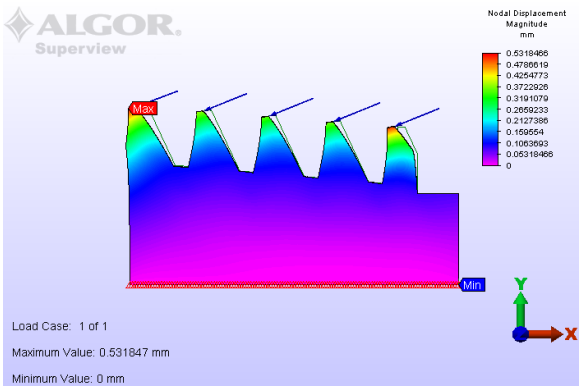

Fig. 18. Displacement distribution – areas of equal displacement. Deformed position of the structure

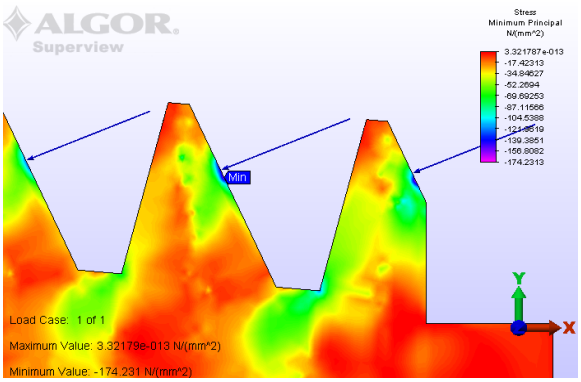

Fig. 21. Detail - Minimum principal stress distribution (compressive stress distribution)

b) Loading in operating

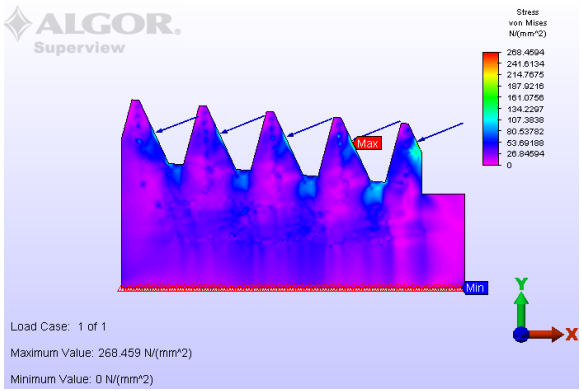

Fig. 19. Equivalent Von Mises stress distribution

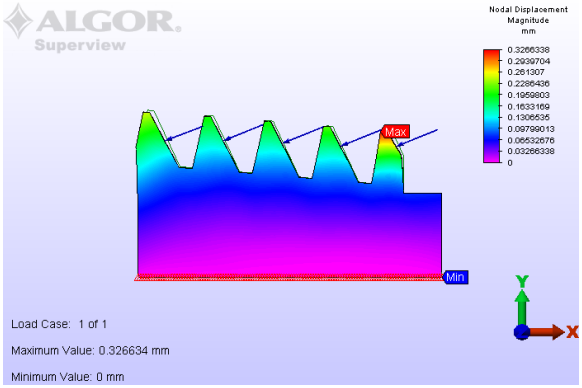

Fig. 22. Displacement distribution – areas of equal displacements. Deformed position of the structure

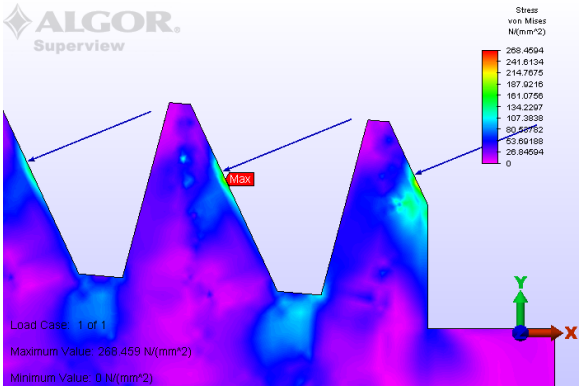

Fig. 20 Detail – Equivalent Von Mises stress distribution in area with high application

Maximum values of tension in the contact points are shown in Table 1

Table 1. Values of stresses in the contact points

Maximum stresses		**Equivalent Von Mises stress σ_{ech} [MPa]**	**Minimum principal stress σ_2 [MPa]**
Case I Bearing flank 10^0	a	387,211	-212,108
	b	228,537	-261,885
Case II Bearing flank 30^0	a	416,813	-245,880
	b	268,459	-174,231

4. Conclusion

Interpreting results based on simulations can be seen:

- For both cases studied, the 10^0 and the 30^0 bearing flank, the maximum stresses produced on the 4th tooth;
- Maximum stresses that occur are beyond allowable resistance of the material the worm-wheel is made of:

$$\sigma_c = 75\,N/mm^2;$$

$$\sigma_r = 100\,N/mm^2$$

- Loading on the contact point was achieved by nodal forces, maximum stresses values resulting directly being nodal point of contact;
- In fact the contact between worm-worm wheel is not as a point but is done on an area;
- The values of stresses in the immediate surrounding nodes are much smaller (Fig.23).

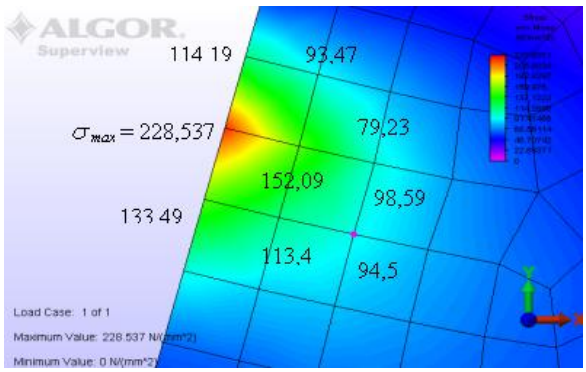

Fig. 23 Von Mises tensions surrounding nodes in contact point of worm-wheel worm

$$\sigma_{ef} \approx 150 - 200\ N/mm^2$$

- However the existing data on the calculated load, the values of power and rotation speed in operation will cause damage on 4th tooth of worm-wheel;
- In the Von Mises stress values is preponderate the compressive and stress σ parts (Table 1, Fig.8, Fig.12, Fig.13, Fig.17, Fig. 21);
- Move the maximum occurs when the first tooth bearing flank is 10^0 and the last tooth when bearing flank is 30^0.

5. References

[1] Brezeanu, L., C., Bica, C., *Modelare si analiza cu elemente finite*, Editura Universitatății "Petru Maior", Tg. Mureș, 2008;

[2] Brezeanu, L., C., Mathe, M., *The Study of the Influences of Cutting Forces on the Edge of Fellow's Cutters through Finite Element Method*, *ISI* Proceedings of the International Conference on Gearing, Transmissions, and Mechanical Systems, Professional Engineering publishing, pp.921-928, ISBN 1 86058 260 53-6 July, 2000, Nottingham, U.K.;

[3] Bucur, B., & Boloș,V., *Experimental study of the thermal limit for the gearbox worm face-gear with reverse tapered pinion*, Proceeding of the 9th International Conference MTeM 2011, Technical University, pp. 53-56, ISBN 978-606-8372-02-0, Cluj-Napoca, October 2011, Gyenge, Cs. (Ed.) Cluj-Napoca, Romania;

[4] Pozdîrcă Al., Kalman Albert, Cheţan P., - *Inventor – Modelare parametrică,* Colecția CAD&CAM – Modul 04, Editura Universitatății "Petru Maior", Tg. Mureș, 2004;

[5] *** ALGOR - *Finite Element Analysis in Practice- Instructor Manual*, Pittburgh, PA, 2004

[6] *** Autodesk INVENTOR Professional, *FEA Module*, CAD-FEM GmbH, 2004.

[7] *** http://www.ptfe.ro/inc/poliamida.pdf